ACS Sustainable Chemistry & Engineering

Research Article

Cite This: ACS Sustainable Chem. Eng. 2019, 7, 13369−13378

pubs.acs.org/journal/ascecg

Multifunctional Urea Cocrystal with Combined Ureolysis and Nitrification Inhibiting Capabilities for Enhanced Nitrogen Management

Luca Mazzei,[†,∥] Valquiria Broll,[†,∥] Lucia Casali,[‡,∥] Manoj Silva,[§] Dario Braga,[‡] Fabrizia Grepioni,*[,‡] Jonas Baltrusaitis,*[,§] and Stefano Ciurli*[,†]

[†]Laboratory of Bioinorganic Chemistry, Department of Pharmacy and Biotechnology, University of Bologna, Viale Giuseppe Fanin 40, 40127 Bologna, Italy

[‡]Dipartimento di Chimica "G. Ciamician", University of Bologna, Via Selmi, 2, 40126 Bologna, Italy

[§]Department of Chemical and Biomolecular Engineering, Lehigh University, 111 Research drive, Bethlehem, Pennsylvania 18015, United States

Supporting Information

ABSTRACT: The novel ternary Zn(II)-thiourea−urea ionic cocrystal [Zn(thiourea)(urea)Cl_2], (ZnTU) has been prepared by both solution and mechanochemical processes and structurally characterized by solid-state methods. ZnTU exhibited improved response properties to water as relative humidity as inherited from thiourea. The results of enzymatic activity measurements provide evidence that ZnTU is effective in modulating urea hydrolysis both in vitro (negatively impacting on the activity of isolated urease) and in vivo (decreasing the ureolytic activity of *Sporosarcina pasteurii*, a widespread soil bacterium), and that Zn(II) is the component of the cocrystal acting as the actual urease inhibitor. Concomitantly, the analysis of the ammonia monooxygenase (AMO) enzymatic activity in *Nitrosomonas europaea*, taken as a representative of soil ammonia-oxidizing bacteria, in the presence of ZnTU reveals that thiourea is the only component of ZnTU able to inhibit ammonia conversion to nitrite. It has also been shown that ZnTU maintains these capabilities when applied to bacterial cultures containing both *S. pasteurii* and *N. europaea* working in tandem. The compound can thus act both as a fertilizer via urea and via the Zn(II) and thiourea components, as a dual action inhibitor of the activities of the enzymes urease and AMO, which are responsible for the negative environmental and economic impact of the agricultural use of urea as soil fertilizer. These results indicate that ZnTU should be considered a novel material to improve N fertilization efficiency, toward a more environment-friendly agricultural practice.

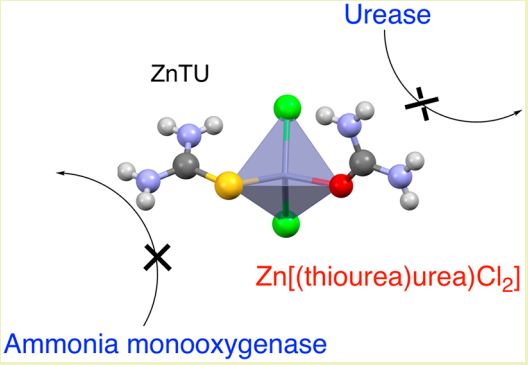

KEYWORDS: *Urease, Ammonia monooxygenase, Urea, Thiourea, Zinc, Soil nitrogen fertilization, Green chemistry*

INTRODUCTION

It has been estimated that the world population will reach 9 billion by the year 2050.[1] In order to sustain the consequential food demand, a 70−100% expansion in global agricultural production will be needed.[2] Nitrogen (N) is an essential nutrient for agriculture and food production,[3] and concerns exist about human impact on the global N cycle.[4,5] Unlike phosphorus (P), N possesses high reactivity in the environment and is prone to significant losses.[5−9] Therefore, novel N management approaches are essential for sustainable soil fertilization and crop productivity.[9]

Urea [$CO(NH_2)_2$] is the most prominent N fertilizer, accounting for more than 60% of the global nitrogen fertilizer use.[10] It is produced via ammonia (NH_3) as an intermediate formed using the Haber process, where hydrogen from natural gas is combined with N_2 obtained from air, under high temperature and pressure in the presence of a catalyst. The process is energy-intensive and uses up to 1% of global energy and ∼4% of natural gas.[11,12] Upon deposition in soil, urea is rapidly hydrolyzed to ammonium (NH_4^+) and bicarbonate (HCO_3^-), a process catalyzed by the nickel-dependent enzyme urease (urea aminohydrolase, EC 3.5.1.5)[13,14] found both as intra- and extra-cellular enzyme.[15] This hydrolysis causes a rapid pH increase in the medium that leads to the formation of gaseous ammonia (NH_3) and consequent N loss from soil.

The NH_4^+ ion formed upon urea hydrolysis serves as a nutrient to plants but additionally undergoes an aerobic nitrification process that leads to the formation of nitrate (NO_3^-) via nitrite (NO_2^-), carried out either by a mutualistic

Received: May 9, 2019
Published: July 10, 2019

DOI: 10.1021/acssuschemeng.9b02607
ACS Sustainable Chem. Eng. 2019, 7, 13369−13378

symbiosis involving ammonia oxidizing bacteria (AOB) and Archaea (AOA) with nitrite-oxidizing bacteria (NOB)[16] or directly by complete ammonia-oxidizing (Comammox) bacteria.[17,18] In all cases, the initial oxidation of NH_4^+ to hydroxyl amine (NH_2OH) is catalyzed by the copper-dependent ammonia monooxygenase (AMO), it is followed by formation of nitrite (NO_2^-) catalyzed by the iron-dependent hydroxylamine oxidoreductase (HAO), and finally by formation of nitrate (NO_3^-), catalyzed by the molybdenum-dependent nitrite oxidoreductase (NIX).[19] Nitrate thus formed in these processes is taken up by plant roots or enters an anaerobic denitrification route, being converted back to nitrite by the Mo-dependent nitrate reductase (NAR); nitrite is then transformed to gaseous forms of N such as nitric oxide (NO), nitrous oxide (N_2O) and eventually dinitrogen (N_2),[20] while a large portion of nitrate is also eventually leached into groundwater.[19]

As a consequence of these processes, as much as 50% of nitrogen fertilizer applied to soil is not used by crops and is lost to the environment, either as gaseous species (NH_3, NO, N_2O, and N_2), some of which significantly contribute to the greenhouse effect[21] and the formation of air particulate matter,[22] or as leached NO_3^-, which is a source of eutrophication.[23−25] This loss represents a very significant economic and environmental cost to farmers specifically, and for society more generally. Development of technologies aimed to increase N use efficiency through environmental N stabilization has been proposed and implemented to varying degrees of success. In particular, methods are highly required that are capable of modulating the N cycle by maintaining this nutrient in a bioavailable form for plants while also limiting environmental mobility.[26,27]

The use of Enhanced Efficiency N fertilizers (EEFs), globally produced on a scale estimated not to exceed ∼3 million metric tons per year, is predicated on the basis of a typical mismatch between nutrient supply and plant demand.[25] There is a wide range of EEFs products in the market, but all have niche applications relative to mainstream products that serve broad scale agriculture: this is due to their high production costs, to the use of unsustainable urea-condensation products such as formaldehyde, and to additional product processing. Therefore, existing EEFs cannot be considered to be a panacea for N agro-environmental management.[28]

An alternative to EEFs are substances acting as inhibitors of the two enzymes that are mainly responsible for the decrease of soil N fertilization efficiency, namely urease and AMO. The urease inhibitor most widely used in agriculture is the organophosphorus compound N-(*n*-butyl)thiophosphoric triamide (NBPT),[29,30] whose detailed inhibition mechanism has been recently elucidated.[31,32] However, some negative effects on soil and crop health have been demonstrated following the use of NBPT.[33−35] On the other hand, the inhibitors most widely used to slow down soil nitrification are nitrapyrin (2-chloro-6-(trichloromethyl) pyridine), dicyandiamide (DCD), and DMPP (3,4-dimethylpyrazole phosphate). However, their mode of action is not known at the molecular level, while other more potent inhibitors are known but not marketed for field applications.[19] One of them, namely thiourea,[36] has been shown to exert a significantly more efficient inhibition of AMO than DCD or nitrapyrin.[37]

New designs, based on urea cocrystals, recently emerged following evidence that urea coordination compounds can reduce N losses from soils. For example, agricultural field tests with NH_4Cl or $ZnSO_4$ have been shown to reduce NH_3 losses from the soil and improve overall nitrogen uptake efficiency when compacted with urea.[38,39] Inhibition of urea reactivity by inorganic acids, such as phosphoric acid, was also shown to decrease NH_3 emissions up to 50% from soils fertilized with urea phosphate ionic cocrystal.[40,41] Significant decrease of NH_3 emissions for urea·$MgSO_4$ cocrystals was similarly observed,[42−44] but the proposed reaction mechanisms were inconclusive. More recent work has expanded this approach by designing urea cocrystals with salts containing Ca^{2+} and Mg^{2+} obtained from parent ionic compounds or via reactive mechanochemistry using the appropriate minerals.[45,46] This approach was further extended to synthesize double salts of NH_4^+ containing HPO_4^{2-}, Ca^{2+}, or Mg^{2+} ions [Ca-$(NH_4)_2(HPO_4)_2{\cdot}H_2O$ dimorph B and $Mg(NH_4)_2(HPO_4)_2{\cdot}4H_2O$ dimorph A] as well as their struvite equivalents [$Ca(NH_4)(PO_4){\cdot}H_2O$ and $Mg(NH_4)(PO_4){\cdot}6H_2O$].[47] Along these lines, the synthesis and characterization of multifunctional urea cocrystalline materials that contained potent urease inhibitors such as catechol[48] and Zn(II),[49] the latter also being an essential micronutrient, were recently reported.

In an effort to develop new materials potentially useful to increase the environmental and economic sustainability of soil N fertilization, we report in this paper on the preparation, structural characterization ,and evaluation of the efficacy of [Zn(thiourea)(urea)Cl_2] (ZnTU), a novel urea cocrystalline material based on the association of urea, thiourea, and $ZnCl_2$, with the goal to provide, simultaneously, a dual enzyme inhibitor of urease [Zn(II)] and AMO (thiourea) together with a high N content organic fertilizer (urea).

EXPERIMENTAL SECTION

Materials. All reagents, including *Canavalia ensiformis* (jack bean) urease (JBU), were purchased from Sigma-Aldrich and used without further purification. *Nitrosomonas europaea* (*N. europaea*, ATCC 19718) was purchased from ATCC (Manassas, USA). *Sporosarcina pasteurii* (*S. pasteurii*, DSM33) was purchased from DSMZ (Braunschweig, Germany).

ZnTU Synthesis and Characterization. *Small Scale Synthesis of ZnTU via Mechanochemistry.* Urea (16.54 mg, 0.28 mmol) was ball-milled with thiourea (20.96 mg, 0.28 mmol) and $ZnCl_2$ (42.49 mg, 0.28 mmol), in a 1:1:1 stoichiometry, with the addition of 50 μL of water, in an agate jar for 60 min at 20 Hz.

Scale-up Synthesis of ZnTU via Slurry. Water (ca. 2 mL) was added dropwise to a physical mixture of urea (2.067 g), thiourea (2.620 g), and $ZnCl_2$ (5.311 g) in a 1:1:1 stoichiometry. When a suspension was obtained that could be easily stirred, the addition of water was interrupted, and the suspension was stirred for 1 day at ambient conditions. The suspension was then filtered under vacuum, and pure ZnTU was recovered as a white crystalline powder. The same procedure was employed to prepare grams of crystalline [$Zn(urea)_2Cl_2$] (ZnU) and [$Zn(thiourea)_2Cl_2$] (ZnT), starting from 1:1 physical mixtures of $ZnCl_2$ (5.315 g):urea (4.604 g) or $ZnCl_2$ (4.720 g):thiourea (5.270 g), respectively.

Single Crystal Growth of ZnTU. Urea (16.54 mg, 0.28 mmol), thiourea (20.96 mg, 0.28 mmol), and $ZnCl_2$ (42.49 mg, 0.28 mmol), in a 1:1:1 stoichiometric ratio, were dissolved in 3 mL of water. Slow evaporation of the solvent at ambient conditions yielded colorless crystals suitable for X-ray diffraction.

Single Crystal X-ray Diffraction. Single crystal data for ZnTU were collected at room temperature with an Oxford Diffraction X′Calibur diffractometer equipped with a graphite monochromator and a CCD detector, using the Mo Kα radiation (λ = 0.71073 Å). Data collection and refinement details are listed in Table 1-SI. The structure of ZnTU was solved using SHELXT-2014[50] and refined on full-matrix F^2 by means of SHELXL-2014[50] implemented in the OLEX 2 software.[51]

DOI: 10.1021/acssuschemeng.9b02607
ACS Sustainable Chem. Eng. 2019, 7, 13369−13378

All non-hydrogen atoms were refined anisotropically. H atoms bound to N atoms were either located from a Fourier map or added in calculated positions, and their position was refined riding on their N atoms. The software Mercury 3.10.16[52] was used for graphical representations and to simulate the powder patterns based on single crystal data. CCDC 1914488 contains the supplementary crystallographic data for this paper. These data are provided free of charge by the Cambridge Crystallographic Data Centre (CCDC).

X-ray Diffraction from Powder. For phase identification purposes, X-ray powder diffraction (XRPD) patterns on ZnTU were collected on a PANalytical X'Pert Pro Automated diffractometer equipped with an X'celerator detector in Bragg−Brentano geometry, using the Cu−Kα radiation (λ = 1.5418 Å) without monochromator in the 5−50° 2θ range (step size 0.033°; time/step: 20 s; Soller slit 0.04 rad, antiscatter slit: 1/2, divergence slit: 1/4 ; 40 mA*40 kV).

Differential Scanning Calorimetry (DSC). DSC traces were recorded using a PerkinElmer Diamond differential scanning calorimeter. All samples (ca. 10 mg of ZnTU, ZnU, ZnT, urea, and thiourea) were placed in open Al-pans. All measurements were conducted in the 40−200 °C temperature range, at a heating rate of 5.00 °C min^{-1}. DSC traces are reported in Figure 1-SI.

Thermogravimetric Analysis (TGA). TGA measurements of all samples (ca. 10 mg of ZnTU, ZnU, ZnT, urea, and thiourea) were performed using a PerkinElmer TGA7 thermogravimetric analyzer, in the 30−300 °C temperature range, under a N_2 gas flow at a heating rate of 5.00 °C min^{-1}. TGA traces are reported in Figure 2-SI.

Solubility Tests. Solubility of urea at room temperature ranges from 1 to 1.2 g mL^{-1}; therefore, a control experiment was conducted in which 1 g of urea was added to a vial and dissolved in 1 mL of bidistilled water. In a second vial, an amount of ZnTU (4.53 g) containing 1 g of urea was added to 1 mL of bidistilled water; the same procedure was applied, for comparison, to solid ZnU and ZnT.

Dynamic Vapor Sorption Experiments. A dynamic vapor sorption (DVS) intrinsic sorption gravimeter (Surface Measurement Systems Ltd., U.S.A.), equipped with a SMS Ultrabalance having a mass resolution of ±0.1 μg, was used to obtain ramping and equilibrium water vapor sorption isotherms. Approximately 5 mg of powder samples were placed in the apparatus using aluminum pans and initially dried over 600 min with a stream of dry nitrogen to establish a dry mass at 25 °C. The dry mass was calculated after the end of the first drying stage with no relative humidity (0% RH). The sorption cycle experiments were performed from 0% to 95% RH in 5% steps in a preprogrammed sequence before decreasing to 0% RH in reverse order. The instrument maintained a constant target RH until the moisture content change per minute (dm/dt) was less than 0.002% over a 10 min period.

Urease and AMO Enzymatic Inhibition by ZnTU. *Bacterial Cells Growth.* *Nitrosomonas (N.) europaea* cells were grown in 1.5 L of freshly prepared ATCC2265 medium, under constant agitation, in the dark, at 26 °C. After 72 h, a time period necessary to reach an optical density (OD_{600}) of 0.06 and a nitrite concentration of ca. 25 μM (according to the Griess assay[53]), cells were harvested by centrifugation at 14,000 *g* for 20 min at 4 °C, washed with a 100 mM sodium phosphate buffer at pH 7.5, also containing 2 mM $MgSO_4$ (NaPB buffer), resuspended in 6 mL of the same buffer and quantified by their total protein content using the biuret assay.[54] Stock solutions with a total protein concentration of ca. 2.5 mg mL^{-1} were prepared.

Sporosarcina (S.) pasteurii cells were grown in 100 mL of a medium containing 20 g L^{-1} yeast extract, 150 mM urea, 1 mM $NiCl_2$, and 130 mM HEPES at pH 7.5, under constant stirring, for 16 h at 26 °C. Cells were harvested by centrifugation at 3000*g* for 5 min at 4 °C, washed three times with NaPB buffer, resuspended in 6 mL of the same buffer, and quantified by their total protein content using the biuret assay.[54] Stock solutions with a total protein concentration of ca. 2.0 mg mL^{-1} were prepared.

Urease Enzymatic Activity Measurement by the pH-stat Method. The activity of jack bean urease (JBU) was determined by using the pH-STAT method.[55] A T1 pH-meter equipped with a 50−14 T electrode (Crison Instruments, Barcelona, ES), was used to record the volume of a 100 mM HCl solution necessary to maintain the reaction at the fixed pH value of 7.5 for 3 min reaction time. In a reference experiment, solution #1 (final volume = 10.00 mL), composed of 9.80 mL of 2 mM 4-(2-hydroxyethyl)-1-piperazineethanesulfonic acid (HEPES) buffer, at pH 7.5, containing 100 mM urea as substrate, was added with solution #2 (0.20 mL) containing 30 nM JBU in the same buffer (0.6 nM final enzyme concentration). The measurement started 0.5 min after enzyme addition in order to get a uniform enzyme/substrate concentration in the reaction vessel. Urease activity was measured as a function of the total volume of 100 mM HCl needed to maintain the pH constant, defining one unit of the enzyme as the amount of urease required to hydrolyze 1 μmol urea per minute of reaction. The same experimental setup was used to measure the activity of JBU in the presence of ZnTU (2, 4, and 8 μM), $ZnCl_2$ (2, 4, and 8 μM), thiourea (8 μM), and an equimolar solution containing $ZnCl_2$ and thiourea (8 μM) dissolved in solution #1. The values for urease activity measured in each experimental condition were normalized with respect to that measured in the reference experiment and plotted, as a percentage, as a function of the concentration of all tested compounds.

Determination of the ureolytic activity of *S. pasteurii* cells was carried out using a modified pH-STAT procedure. In a reference experiment, *S. pasteurii* cells, resuspended in NaPB buffer, were diluted in deionized water to a final 10 mL volume of 10 mM sodium phosphate buffer, at pH 7.5. The total protein content of *S. pasteurii* cells in the assay was 1 mg. The reaction was started after 2 min preincubation by adding urea to a final 25 mM concentration, and the extent of the ammonification process by *S. pasteurii* was estimated in the following 20 min by measuring the volume of a 100 mM HCl solution needed to maintain the pH of the reaction at the constant value of 7.5. Following the same procedure, the ammonification activity of *S. pasteurii* cells was determined in the presence of 8 μM ZnTU, thiourea, or $ZnCl_2$. The results were normalized with respect to the ammonification extent estimated in the reference experiment and shown as percentage values. All experiments were conducted in triplicates at 25 °C and under constant stirring.

Nitrosomonas Europaea Ammonia Mono-oxygenase Activity Measurement by O_2 Consumption. Consumption of dioxygen (O_2) by *N. europaea* cells was determined using a Clark-type polarographic electrode (Vernier, Oregon, USA) and recording the data using a LabQuest2 sensor data collection system (Vernier, Oregon, USA).[56,57] The reaction mixture (final volume = 5 mL) was composed of 10 mM $(NH_4)_2SO_4$ dissolved in NaPB buffer. After a 3 min pre-equilibration period, the reaction was initiated by addition of a proper volume of cells in the assay, providing a total protein content of ca. 0.5 mg. The traces of recorded O_2 concentration vs time (see Figure 3-SI for a representative plot of the raw data) were integrated over time to obtain the total amount of O_2 consumed by *N. europaea* during the 20 min reaction. For this purpose, the trace describing the O_2 concentration vs time, recorded in the absence of substrate, was used as the baseline for the integration procedure. A typical amount of O_2 consumed by *N. europaea* in this assay was ca. 35 μmoles over 20 min of reaction (reference experiment).

Measurements of O_2 consumption by *N. europaea* cells in the presence of ZnTU (2, 4, and 8 μM), thiourea (2, 4, and 8 μM), urea (8 μM), $ZnCl_2$ (8 μM), and an equimolar (8 μM) solution of thiourea, urea and $ZnCl_2$ were performed using the same experimental setup. All measurements were normalized with respect to the O_2 consumption measured in the reference experiment and plotted, as a percentage, as a function of the amount of the tested compounds. All experiments were conducted in triplicates, in the dark, at 25 °C and under constant stirring.

Nitrosomonas Europaea Ammonia Mono-oxygenase Activity Measurement by NO_2^- Production. Nitrite (NO_2^-) production by *N. europaea* cells was spectrophotometrically determined through the Griess test[53] using a Cary 60 UV−vis spectrophotometer (Agilent, CA, USA). The reaction mixture (final volume = 5 mL) was composed of 50 μM $(NH_4)_2SO_4$ dissolved in NaPB buffer. Nitrite production by *N. europaea* was started upon addition of the cells to the reaction mixture. The concentration of cells used for each

DOI: 10.1021/acssuschemeng.9b02607
ACS Sustainable Chem. Eng. 2019, 7, 13369−13378

experiment was the same as that needed for the corresponding O_2 consumption experiment. The reaction was incubated for 60 min and then treated for 30 min with the Griess reagent, followed by measurements of the absorbance at 548 nm (reference experiment). The same procedure was carried out in the presence of ZnTU (2, 4, and 8 μM), thiourea (2, 4, and 8 μM), urea (8 μM), $ZnCl_2$ (8 μM), and an equimolar (8 μM) solution of thiourea, urea and $ZnCl_2$. For each experiment, a corresponding data set was recorded in the absence of either the substrate or any compound tested, and subsequently subtracted to the original experiment in order to minimize absorbance contribution by either *N. europaea* cells or the tested compounds. All measurements were normalized with respect to the amount of nitrite produced measured in the reference experiment and plotted, as a percentage, as a function of the amount of the tested compounds. All experiments were conducted in triplicates, in the dark, at 25 °C and under constant stirring.

Urea Hydrolysis and O_2 Consumption by Sporosarcina pasteurii and Nitrosomonas europaea: Tandem Experiments. The capability of *S. pasteurii* to hydrolyze urea and yield HCO_3^- and NH_4^+ was exploited to test the ability of *N. europaea* cells to oxidize ammonia to nitrite, in a tandem experiment using a medium containing both microorganisms. In particular, the extent of urea ammonification by *S. pasteurii* and of O_2 consumption by *N. europaea* were measured in a mixture where *S. pasteurii* and *N. europaea* cells, both resuspended in NaPB buffer, were diluted in deionized water to a final 10 mL volume of 10 mM sodium phosphate buffer, at pH 7.5. The total protein content for *S. pasteurii* and *N. europaea* cells in the assay was ca. 1 mg each. The reaction was started after 2 min preincubation by adding urea to a final 25 mM concentration. Both ammonification and O_2 consumption rates were simultaneously monitored for 20 min by following the same experimental procedure as described above. Ammonification and O_2 consumption processes were also determined in the presence of 8 μM ZnTU, thiourea, or $ZnCl_2$. The results were normalized with respect to the corresponding reference experiment and represented as percentage values. All experiments were conducted in triplicates, in the dark, at 25 °C and under constant stirring.

RESULTS

Structural Characterization of ZnTU. The molecular structure of ZnTU in the solid state is shown in Figure 1, together with the molecular structures of the analog compounds containing two urea (ZnU, refcode ZZZDNU01) or two thiourea (ZnT, refcode CLSTUZ02) molecules bound to $ZnCl_2$. Figure 2 shows a comparison of the main hydrogen bonding motifs in the three solids. Bifurcated interactions of the $NH_2\cdots Cl$ type are common to all three crystals and involve both urea and thiourea NH_2 groups [$N(H_2)\cdots Cl$ distances 3.391−3.533, 3.495−3.514, and 3.385(5)−3.516(5) Å for ZnU, ZnT, and ZnTU, respectively]. On the contrary, the cyclic hydrogen-bonded dimers, formed by the urea molecules in ZnU [$N(H_2)\cdots O$ distance 3.098 Å] and by the thiourea molecules in ZnT [$N(H_2)\cdots S$ distance 3.646 Å], involve only the urea molecules in ZnTU [$N(H_2)\cdots O$ distance 3.018(6) Å].

The structural identity of the product of the crystallization and of the product of the solid-state synthesis carried out by cogrinding the three pure solid reactants (albeit with the addition of a small quantity of water) was verified by comparing the XRPD patterns calculated on the basis of the single crystal structure and the experimental pattern measured on the crystalline powder (Figure 3).

Comparative Thermal Stability of ZnTU. A comparison of the DSC traces for urea, thiourea, ZnTU, ZnU, and ZnT (Figure 1-SI) shows that cocrystallization of the organic molecules with $ZnCl_2$ significantly reduces the melting point (peak temperatures), especially in the three-components cocrystal ZnTU [100(1) °C] as compared to the melting

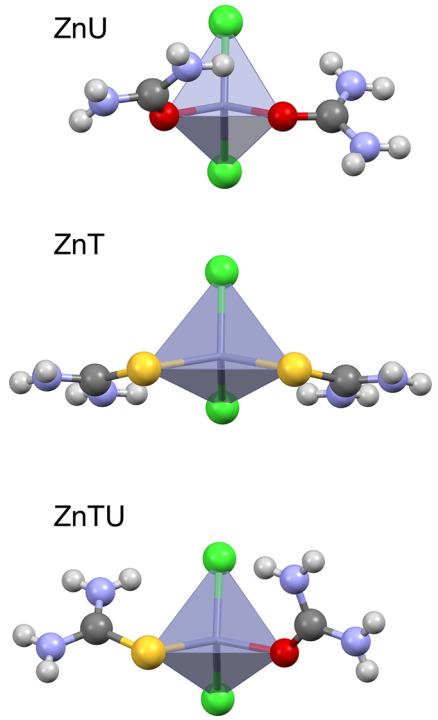

Figure 1. Comparison of the molecular structures for crystalline ZnU (refcode ZZZDNU01), ZnT (refcode CLSTUZ02) and ZnTU (refcode 1914488). Color code: Zn, black; O, red; S, yellow; C, dark gray; N, blue; H, light gray; Cl, green.

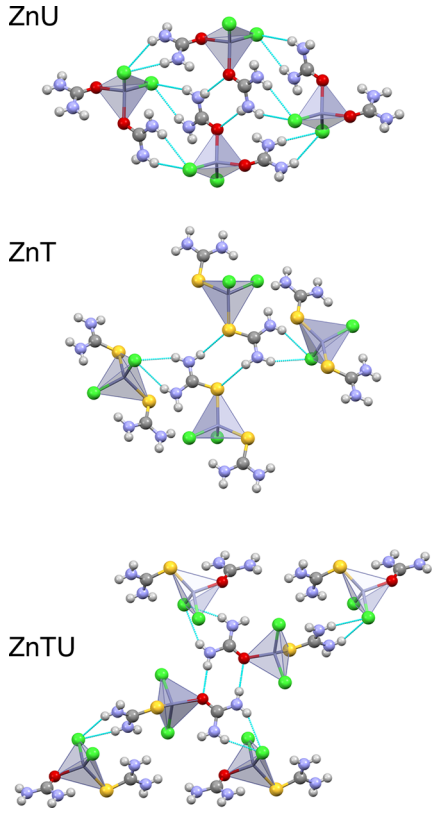

Figure 2. Comparison of the hydrogen bonding motifs in crystalline ZnU (top), ZnT (middle), and ZnTU (bottom). Color code: Zn, black; O, red; S, yellow; C, dark gray; N, blue; H, light gray; Cl, green.

DOI: 10.1021/acssuschemeng.9b02607
ACS Sustainable Chem. Eng. 2019, 7, 13369−13378

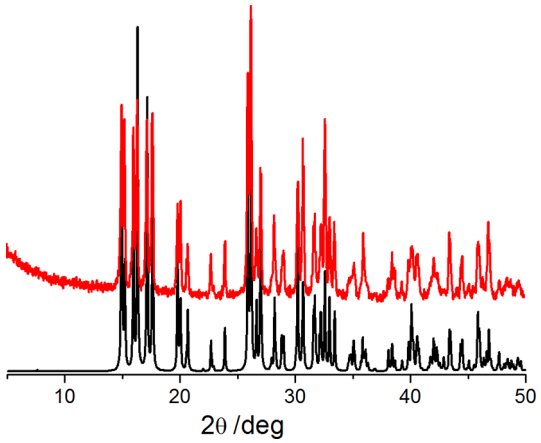

Figure 3. Comparison between the experimental pattern measured for ZnTU as obtained by solid-state synthesis (red line) and the pattern calculated on the basis of the single crystal structure (black line).

points for urea [137(1) °C], thiourea [179(1) °C], ZnU [124(1) °C], and ZnT [157(1) °C]. No thermal event is observed in the DSC trace of ZnTU prior to melting. The TGA trace for ZnTU shows that the compound is stable up to 100 °C (see Figure 2-SI).

Solubility Tests. The solubility of urea in water, when associated with $ZnCl_2$ and thiourea, was about a third of that observed for pure urea in water: of the 4.53 g of ZnTU (containing 1 g of urea) only 1.71 g were dissolved in 1 mL of water, corresponding to a solubility in water of ca. 0.38 g mL^{-1} for urea in ZnTU. The residual undissolved solid was filtered, dried and weighed, resulting in ca. 2.82 g of powder material, which was analyzed via X-ray powder diffraction and found to be a mixture of ZnTU and ZnT (see Figure 4-SI). The solubility of ZnTU in water was then compared to that of the cocrystals ZnU and ZnT. While 1 g of ZnU is totally dissolved in water, this is not the case with the same weight of ZnT and ZnTU (see Figure 4), suggesting that the presence of thiourea

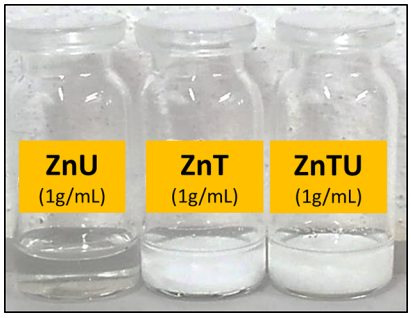

Figure 4. Comparison of ZnU, ZnT, and ZnTU solubility in water; all vials contain the same amount of urea.

drastically reduces the solubility of crystalline ZnTU due to formation of the less soluble ZnT (solubility of ZnT ca. 0.46 mg mL^{-1} vs 1.71 g mL^{-1} for ZnTU).

Stability Tests. A sample of crystalline ZnTU was kept in an open flask at ambient conditions for six months. A powder diffractogram was recorded immediately before storage and after six months. As it can be seen from Figure 5-SI, the two patterns are largely superimposable, implying that ZnTU is fairly stable toward humidity absorption from the atmosphere, even though a few additional peaks (which we have not yet been able to characterize) are present in the 6-months sample.

Stability of crystalline ZnTU, ZnU, and ZnT toward controlled humidity was tested by storing the solids for 3 days in a chamber kept at room temperature and containing a saturated aqueous solution of KCl (relative humidity 82%). At the end of the 3 days ZnU had absorbed water and had turned into an aqueous solution; ZnTU, on the contrary, showed the same behavior as ZnT, i.e., remained essentially unchanged. This suggests that urea in ZnTU is stabilized with respect to urea in ZnU (see Figure 6-SI).

Dynamic Vapor Sorption (DVS) Analysis. The amount of adsorbed water and response to changes in relative humidity by urea, thiourea and ZnTU were investigated using constant temperature adsorption/desorption experiments by varying the relative humidity (RH), defined as $RH(\%) = \frac{P}{P_o} \times 100$ (where P_o is the saturated vapor pressure of water at 298 K and 1 atm and P is the actual water pressure at the same temperature and pressure). The results, shown in Figure 5, show that water

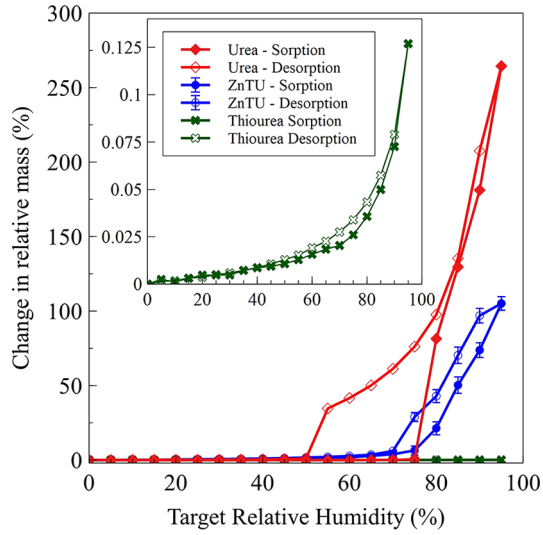

Figure 5. Adsorption/desorption branches of RH on urea, ZnTU, and thiourea.

uptake remained negligible during the hydration of urea, until a deliquescence phase transition ensues at 74% RH, indicating a sharp size increase and liquid layer formation. Subsequently, with further increases in RH, the aqueous droplet underwent continuous hygroscopic growth. During the dehydration process, the representative urea particle showed a two-stage phase transition: the liquid droplet decreased gradually in size with decreasing RH down to 74% and became supersaturated with respect to urea; with a further decrease in RH, an effloresced particle was formed at 50% RH. These data are consistent with previous measurements.[48] Thiourea, on the other hand, exhibited nearly no RH adsorption, with negligible mass increase even at high (>70% RH) values where typically deliquescence of hygroscopic materials appears, and essentially no hysteresis (inset of Figure 5). Finally, ZnTU appeared to inherit the hygroscopic properties of both parent materials (urea and $ZnCl_2$), consistently with qualitative data shown in Figure 4. Specifically, the total adsorbed water as RH amount decreased about 2.5 times at ∼90% RH as compared to urea, while hysteresis decreased significantly. These results suggest

DOI: 10.1021/acssuschemeng.9b02607
ACS Sustainable Chem. Eng. 2019, 7, 13369−13378

that the deliquescence of ZnTU is decreased because of the presence of thiourea in the material. This is further supported by the observation that ZnU and ZnT largely inherits the water sorption properties of urea and thiourea, respectively (Figure 7-SI). However, differently from solution studies, RH did not induce decomposition of ZnTU into any binary parent compounds as indicated by the absence of of new peaks in the absorption desorption curves.

Urease Inhibition by ZnTU through in Vitro and in Vivo Enzymatic Activity Measurements. Measurements of urease (JBU) activity revealed the concentration-dependent urease inhibition property of ZnTU (Figure 6A). In particular, at the lowest concentration of ZnTU used, ca. 30% activity loss is observed, the latter increasing to ca. 80% at the highest concentration tested (8 μM). A control experiment, carried out using 8 μM thiourea, showed that this single component does not exert any inhibition effect, while an 8 μM mixture of $ZnCl_2$ and thiourea showed the same inhibition strength as ZnTU (Figure 6B). The concentration-dependent inhibition of JBU by $ZnCl_2$ (Figure 6B) confirmed the latter as the sole active component of ZnTU as the urease inhibitor.

Determination of the enzymatic hydrolysis of urea using *S. pasteurii* cells, investigated in the absence or presence of 8 μM ZnTU indicated that the latter is able to inhibit ca. 80% of the ureolytic activity of *S. pasteurii* (Figure 6C). Control experiments carried out using 8 μM $ZnCl_2$ and thiourea further showed that while $ZnCl_2$ has an inhibition effect on ammonification by *S. pasteurii* comparable to that of ZnTU, thiourea does not affect the microbial ability to hydrolyze urea (Figure 6C).

Ammonia Mono-oxygenase Inhibition by ZnTU through in Vivo Enzymatic Activity Measurements. The oxidation of ammonia to nitrite by *N. europaea* is a strictly aerobic process so that the ability of ZnTU to reduce the nitrification process was monitored by measuring the O_2 consumption by *N. europaea* cells in the presence of increasing amounts of ZnTU. As shown in Figure 7A, ZnTU negatively affects the ability of *N. europaea* cells to consume O_2 in a dose-dependent manner, causing a decrease of 40% and 75% at the lowest and highest ZnTU concentration tested. The oxidation of ammonia by AMO from *N. europaea* produces hydroxylamine, that is in turn oxidized to nitrite by hydroxylamine oxidoreductase (HAO). To establish whether ZnTU is able to reduce the amount of nitrite produced as part of the nitrification process, *N. europaea* cells were incubated with increasing concentrations of ZnTU and the concentration of produced nitrite was determined (Figure 7B). The dose/response profile of ZnTU on nitrite formation resulted in a *ca.* 30% and 75% decrease of the amount detected at the lowest and the highest tested ZnTU concentrations, respectively.

In order to determine the possible contribution to AMO inhibition by the single species present in the ZnTU cocrystal, additional experiments were carried out using 8 μM of a stoichiometric mixture of $ZnCl_2$, urea and thiourea, as well as $ZnCl_2$ and urea tested separately using the O_2 consumption (Figure 7C) and the nitrite production (Figure 7D) assays. In both assays, the mixture shows an effect comparable to that of 8 μM ZnTU, whereas $ZnCl_2$ and urea do not show any inhibitory effect. Therefore, thiourea was further investigated at 2, 4, and 8 μM to verify its contribution to the dose-dependent effect observed for ZnTU. The latter hypothesis was confirmed by the concentration-dependent profiles shown in Figure 7C,D.

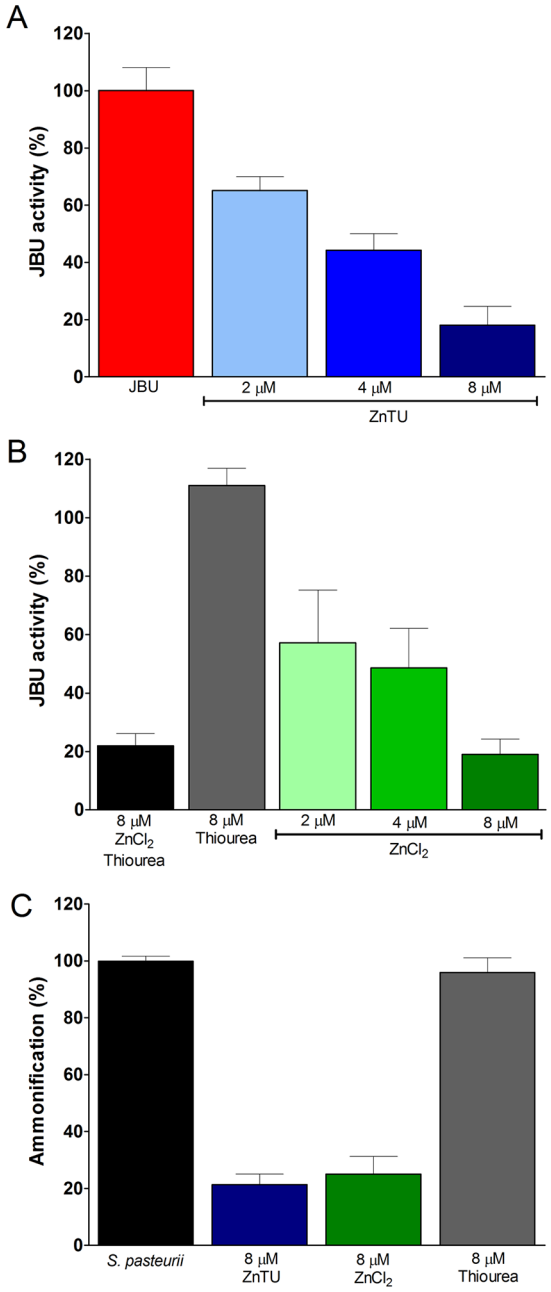

Figure 6. (A) Residual percentage activity of jack bean urease (JBU) at pH 7.5, as a function of increasing concentrations of ZnTU. The red bar corresponds to the reference experiment performed in the absence of ZnTU, while the light blue, blue and dark blue bars correspond to urease activity measured in the presence of 2, 4, and 8 μM ZnTU, respectively. (B) Residual percentage activity of jack bean urease (JBU), at pH 7.5, as a function of 8 μmol L^{-1} mixture of thiourea and $ZnCl_2$ (black bar), 8 μmol L^{-1} thiourea (dark gray bar) and 2, 4, and 8 μmol L^{-1} $ZnCl_2$ (light green, green and dark green bars). All values are normalized with respect to the reference experiment.

***N. europaea* and *S. pasteurii* Correlated Enzymatic Activity.** Production of ammonia from the enzymatic hydrolysis of urea carried out by *S. pasteurii* was exploited in a tandem experiment in which *S. pasteurii* and *N. europaea* cells were simultaneously present, to produce the substrate for the ammonia mono-oxygenase (AMO) enzyme, active in *N. europaea*. This assay was used to test the *in vivo* inhibition

DOI: 10.1021/acssuschemeng.9b02607
ACS Sustainable Chem. Eng. 2019, 7, 13369−13378

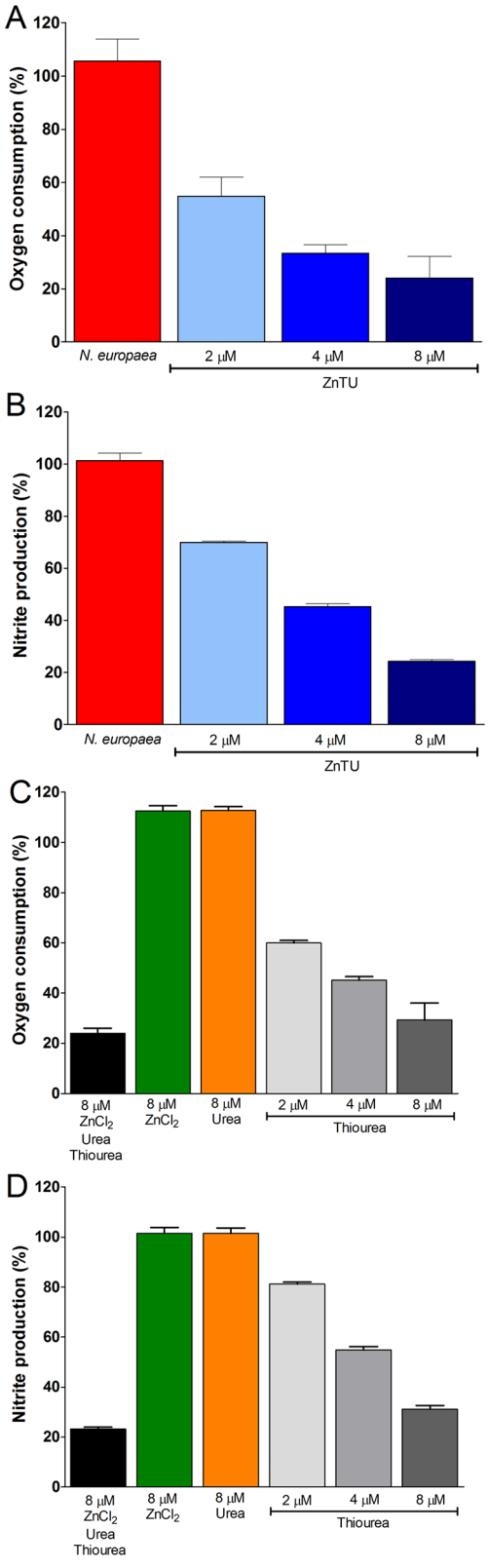

Figure 7. (A) Percentage O_2 consumption and (B) nitrite production by *N. europaea*, at pH 7.5, as a function of increasing concentrations of ZnTU. The red bar corresponds to the reference experiment performed in the absence of ZnTU, while the light blue, blue, and dark blue bars correspond to oxygen consumption or nitrite production measured in the presence of 2, 4, and 8 μM ZnTU, respectively. (C) Percentage of oxygen consumption and (D) nitrite production by *Nitrosomonas europaea*, at pH 7.5, as a function of 8 μmol L^{-1} mixture of thiourea, urea and $ZnCl_2$ (black bar), 8 μmol L^{-1} $ZnCl_2$ (dark green bar), 8 μmol L^{-1} urea (orange bar), and 2, 4, and 8 μmol L^{-1} thiourea (light gray, gray, and dark gray bars). All values are normalized with respect to the reference experiment.

properties of ZnTU on both the ammonification and nitrification processes carried out by the two organisms present in the same reaction mixture. In Figure 8A, the

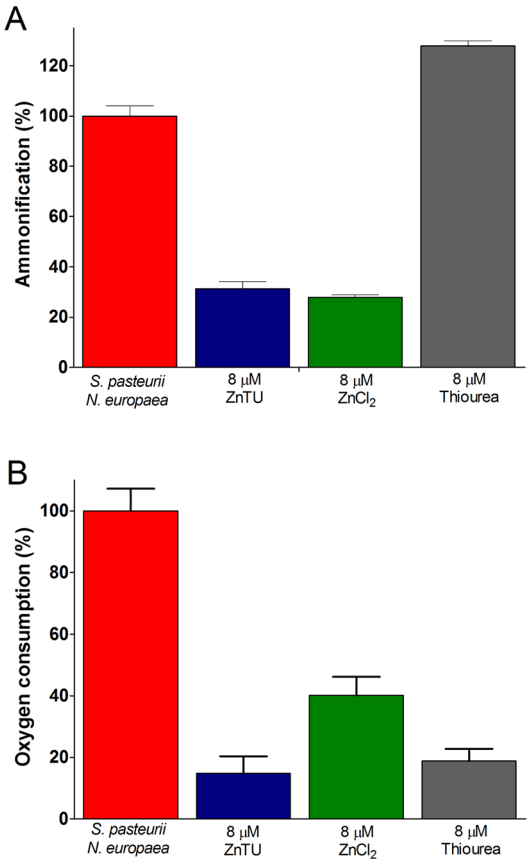

Figure 8. (A) Percentage ammonification by *S pasteurii*, at pH 7.5, as a function of 8 μM ZnTU, $ZnCl_2$ or thiourea. (B) Percentage ammonification and (C) percentage O_2 consumption determined in the tandem experiment in the presence of both *S pasteurii* and *N. europaea*, at pH 7.5, as a function of 8 μM ZnTU, $ZnCl_2$ or thiourea. The red and black bars correspond to the analysis performed in the absence of ZnTU on *S. pasteurii* and *N. europaea*, and on *S. pasteurii* only, respectively. The dark blue, dark green, and dark gray bars correspond to 8 μM of ZnTU, 8 μM of $ZnCl_2$ and 8 μM of thiourea, respectively.

ammonification process performed by *S. pasteurii* in the presence of *N. europaea* and in the absence of ZnTU demonstrated that, in this assay, *S. pasteurii* is still able to process urea even in the presence of *N. europaea*. Moreover, the effect of ZnTU reflects the same behavior as that previously described when *S. pasteurii* was probed alone (Figure 6C), with 8 μM ZnTU able to inhibit almost 70% of the original amount. As expected, 8 μM $ZnCl_2$ and thiourea (Figure 8A) also reproduce the results previously determined for *S. pasteurii* alone (Figure 6C), with the presence of thiourea increasing the percentage of ammonification because this compound can act as urease substrate in addition to urea itself.

DOI: 10.1021/acssuschemeng.9b02607
ACS Sustainable Chem. Eng. 2019, 7, 13369−13378

The amount of O_2 consumed by the two bacteria in the absence or in the presence of ZnTU was also measured (Figure 8B). The ammonia oxidation process performed by *N. europaea* in the presence of *S. pasteurii* and in the absence of ZnTU demonstrated that, in this assay, *N. europaea* can use the ammonia produced by *S. pasteurii* as a substrate for its metabolic pathways. *S. pasteurii* alone shows a negligible contribution on the O_2 consumption with respect to the amount measured for the two bacteria (not shown). ZnTU negatively affects the O_2 consumption by *N. europaea* in the mixture by *ca.* 80% with respect to the control (Figure 8B), confirming the observation for *N. europaea* alone (Figure 7A). Thiourea drastically reduces O_2 consumption to a similar range as observed for ZnTU (Figure 8B), whereas it has no effect on urea hydrolysis performed by *S. pasteurii* in the presence of *N. europaea* (Figure 8A). This behavior can be explained by the fact that thiourea, in the range of concentrations tested, is able to solely affect AMO activity. $ZnCl_2$ shows less severe, but still pronounced effect on *N. europaea* use of O_2 (Figure 8B) This result is not directly ascribable to an effect of $ZnCl_2$ on the consumption of O_2 by *N. europaea* itself, as previously reported (Figure 7C), but it rather highlights the inhibitory action of $ZnCl_2$ on the ammonification process by *S. pasteurii* (see Figure 6C) that causes a depletion of ammonia in solution, and indirectly results in a decrease of the actual concentration of substrate available for the nitrification process by *N. europaea*. These data suggest that ZnTU under moist environments inherits intermediate response properties of the parent compounds in agreement with the determined crystal structure and its composition.

DISCUSSION

With this paper, we have reported the facile preparation, via mechanochemistry, of a novel three-component cocrystalline system with useful properties in terms of soil N fertilization and soil enzyme inhibition. ZnTU is capable of providing urea to the soil while reducing, at the same time, the activities of the enzymes urease and ammonia monooxygenase (AMO), which are responsible for the decrease of the urea-based N fertilization efficiency. The novel compound has been fully characterized and the results of diffraction, calorimetric, dynamic vapor sorption, and solubility experiments have been analyzed also in the light of the behavior of analog ZnU and ZnT, containing either organic moiety linked to Zn(II).

A comparative analysis of urease enzymatic assays performed using the pure enzyme (JBU) in the presence of ZnTU or its single components or cells of a ureolytic organism (*S. pasteurii*) reveals a similar concentration-dependent behavior if ZnTU and Zn(II) are considered, while no effect is observed in the presence of thiourea (Figure 6). These results indicate that ZnTU is a compound effective in modulating the ammonification effect both in vitro (negatively impacting on the activity of urease) and in vivo (decreasing *S. pasteurii* ureolytic activity), and that Zn(II) is the component of the cocrystal acting as the actual inhibitor. Analogously, a similar analysis carried out by comparing the AMO enzymatic activity in *N. europaea* in the presence of ZnTU (Figure 7) reveals that thiourea is the only component of ZnTU able to inhibit the activity of AMO. Finally, the analysis of the effects of ZnTU on a combination of *S. pasteurii* and *N. europaea*, representative of soil ureolytic and ammonia-oxidizing bacteria, respectively, reveals that the cocrystalline material maintains the capability, with its single components, to inhibit both urease and ammonia oxidation activities. To the best of the authors' knowledge, this is the first time that such a tandem experiment has been attempted in order to model soil activity.

In conclusion, the novel ternary urea-thiourea ionic cocrystal $[Zn(thiourea)(urea)Cl_2]$, (ZnTU) appears to meet the requirement for a new material potentially useful to increase the environmental and economic sustainability of soil N fertilization, combining the N fertilizer properties with those of inhibitors of the enzymes urease and ammonia monooxygenase (AMO). Besides, ZnTU appears to be a promising material for utilization in the field because, inter alia, the compound can be prepared by environmentally friendly and economically advantageous mechanochemical methods.

ASSOCIATED CONTENT

Supporting Information

The Supporting Information is available free of charge on the ACS Publications website at DOI: 10.1021/acssuschemeng.9b02607.

Crystallographic data and details of measurements for ZnTU; differential scanning calorimetric and thermogravimetric traces for urea, thiourea, ZnU, ZnT, and ZnTU; representative data of oxygen consumption by *S. pasteurii* and *N. europaea*; powder X-ray diffraction patterns of ZnT and ZnTU; water absorption by solid portions of ZnTU, ZnU, and ZnT; adsorption/desorption curves of relative humidity for urea, ZnU, thiourea, and ZnT (PDF)

AUTHOR INFORMATION

Corresponding Authors

*E-mail: fabrizia.grepioni@unibo.it.
*E-mail: job314@lehigh.edu.
*E-mail: stefano.ciurli@unibo.it.

ORCID

Luca Mazzei: 0000-0003-1335-9365
Dario Braga: 0000-0003-4162-4779
Fabrizia Grepioni: 0000-0003-3895-0979
Jonas Baltrusaitis: 0000-0001-5634-955X
Stefano Ciurli: 0000-0001-9557-926X

Author Contributions

‖L.M., V.B., and L.C. contributed equally to the work.

Notes

The authors declare no competing financial interest.

ACKNOWLEDGMENTS

This work was supported by the National Science Foundation under Grant Number CHE-1710120 (to J.B.) and by the University of Bologna (RFO scheme, to D.B., F.G., and S.C.). L.M. was supported by the University of Bologna and by CIRMMP (Consorzio Interuniversitario di Risonanze Magnetiche di Metallo-Proteine). V.B. was supported by CIRMMP.

REFERENCES

(1) Evans, A. *The Feeding of the Nine Billion: Global Food Security*; Chatham House: London, 2009.
(2) Godfray, H. C. J.; Beddington, J. R.; Crute, I. R.; Haddad, L.; Lawrence, D.; Muir, J. F.; Pretty, J.; Robinson, S.; Thomas, S. M.;

DOI: 10.1021/acssuschemeng.9b02607
ACS Sustainable Chem. Eng. 2019, 7, 13369−13378

Toulmin, C. Food security: the challenge of feeding 9 billion people. *Science* **2010**, *327* (5967), 812−818.
(3) Roy, R. N.; Finck, A.; Blair, G. J.; Tandon, H. L. S. *Plant Nutrition for Food Security*; Food and Agriculture Organization of the United Nations: Rome, 2006; p 348.
(4) Galloway, J. N.; Dentener, F. J.; Capone, D. G.; Boyer, E. W.; Howarth, R. W.; Seitzinger, S. P.; Asner, G. P.; Cleveland, C. C.; Green, P. A.; Holland, E. A.; Karl, D. M.; Michaels, A. F.; Porter, J. H.; Townsend, A. R.; Vöosmarty, C. J. Nitrogen Cycles: Past, Present, and Future. *Biogeochemistry* **2004**, *70* (2), 153−226.
(5) Erisman, J. W.; Sutton, M. A.; Galloway, J.; Klimont, Z.; Winiwarter, W. How a century of ammonia synthesis changed the world. *Nat. Geosci.* **2008**, *1*, 636.
(6) Duce, R. A.; LaRoche, J.; Altieri, K.; Arrigo, K. R.; Baker, A. R.; Capone, D. G.; Cornell, S.; Dentener, F.; Galloway, J.; Ganeshram, R. S.; Geider, R. J.; Jickells, T.; Kuypers, M. M.; Langlois, R.; Liss, P. S.; Liu, S. M.; Middelburg, J. J.; Moore, C. M.; Nickovic, S.; Oschlies, A.; Pedersen, T.; Prospero, J.; Schlitzer, R.; Seitzinger, S.; Sorensen, L. L.; Uematsu, M.; Ulloa, O.; Voss, M.; Ward, B.; Zamora, L. Impacts of Atmospheric Anthropogenic Nitrogen on the Open Ocean. *Science* **2008**, *320* (5878), 893.
(7) Canfield, D. E.; Glazer, A. N.; Falkowski, P. G. The Evolution and Future of Earth's Nitrogen Cycle. *Science* **2010**, *330* (6001), 192.
(8) Oikawa, P. Y.; Ge, C.; Wang, J.; Eberwein, J. R.; Liang, L. L.; Allsman, L. A.; Grantz, D. A.; Jenerette, G. D. Unusually high soil nitrogen oxide emissions influence air quality in a high-temperature agricultural region. *Nat. Commun.* **2015**, *6*, 8753.
(9) Zhang, X.; Davidson, E. A.; Mauzerall, D. L.; Searchinger, T. D.; Dumas, P.; Shen, Y. Managing nitrogen for sustainable development. *Nature* **2015**, *528*, 51.
(10) Prud'homme, M. *Global Fertilizer Supply and Trade*; Dubai, UAE, 2016.
(11) Patil, B. S.; Wang, Q.; Hessel, V.; Lang, J. Plasma N_2-fixation: 1900−2014. *Catal. Today* **2015**, *256*, 49−66.
(12) Baltrusaitis, J. Sustainable Ammonia Production. *ACS Sustainable Chem. Eng.* **2017**, *5* (11), 9527−9527.
(13) Maroney, M. J.; Ciurli, S. Nonredox nickel enzymes. *Chem. Rev.* **2014**, *114* (8), 4206−28.
(14) Mazzei, L.; Musiani, F.; Ciurli, S. Urease. In *The Biological Chemistry of Nickel*; Zamble, D., Rowin′ska-Żyrek, M., Kozłowski, H., Eds.; Royal Society of Chemistry: London, 2017; pp 60−97.
(15) Burns, R. G. Interaction of enzymes with soil mineral and organic colloids. In *Interactions of soil minerals with natural organics and microbes*; Huang, P. M. a. S. M., Ed.; Soil Science Society of America: Madison, WI, 1986; Vol. Special publication n.17, pp 429−452.
(16) Stein, L. Y.; Klotz, M. G. The nitrogen cycle. *Curr. Biol.* **2016**, *26* (3), R94−8.
(17) Daims, H.; Lebedeva, E. V.; Pjevac, P.; Han, P.; Herbold, C.; Albertsen, M.; Jehmlich, N.; Palatinszky, M.; Vierheilig, J.; Bulaev, A.; Kirkegaard, R. H.; von Bergen, M.; Rattei, T.; Bendinger, B.; Nielsen, P. H.; Wagner, M. Complete nitrification by *Nitrospira* bacteria. *Nature* **2015**, *528*, 504.
(18) van Kessel, M. A. H. J.; Speth, D. R.; Albertsen, M.; Nielsen, P. H.; Op den Camp, H. J. M.; Kartal, B.; Jetten, M. S. M.; Lücker, S. Complete nitrification by a single microorganism. *Nature* **2015**, *528*, 555.
(19) Beeckman, F.; Motte, H.; Beeckman, T. Nitrification in agricultural soils: impact, actors and mitigation. *Curr. Opin. Biotechnol.* **2018**, *50*, 166−173.
(20) Maia, L. B.; Moura, J. J. How biology handles nitrite. *Chem. Rev.* **2014**, *114* (10), 5273−357.
(21) Coskun, D.; Britto, D. T.; Shi, W.; Kronzucker, H. J. Nitrogen transformations in modern agriculture and the role of biological nitrification inhibition. *Nature Plants* **2017**, *3*, 17074.
(22) Paulot, F.; Jacob, D. J. Hidden cost of U.S. agricultural exports: particulate matter from ammonia emissions. *Environ. Sci. Technol.* **2014**, *48* (2), 903−908.
(23) Tilman, D.; Fargione, J.; Wolff, B.; Antonio, C.; Dobson, A.; Howarth, R.; Schindler, D.; Schlesinger, W. H.; Simberloff, D.; Swackhamer, D. Forecasting Agriculturally Driven Global Environmental Change. *Science* **2001**, *292* (5515), 281.
(24) Galloway, J. N.; Cowling, E. B. Reactive Nitrogen and The World: 200 Years of Change. *Ambio* **2002**, *31* (2), 64−71.
(25) Chen, D.; Suter, H.; Islam, A.; Edis, R.; Freney, J. R.; Walker, C. N. Prospects of improving efficiency of fertiliser nitrogen in Australian agriculture: a review of enhanced efficiency fertilisers. *Aust. J. Soil Res.* **2008**, *46* (4), 289−301.
(26) Galloway, J. N.; Aber, J. D.; Erisman, J. W.; Seitzinger, S. P.; Howarth, R. W.; Cowling, E. B.; Cosby, B. J. The Nitrogen Cascade. *BioScience* **2003**, *53* (4), 341−356.
(27) Lassaletta, L.; Billen, G.; Grizzetti, B.; Anglade, J.; Garnier, J. 50 year trends in nitrogen use efficiency of world cropping systems: the relationship between yield and nitrogen input to cropland. *Environ. Res. Lett.* **2014**, *9* (10), 105011.
(28) Li, T.; Zhang, W.; Yin, J.; Chadwick, D.; Norse, D.; Lu, Y.; Liu, X.; Chen, X.; Zhang, F.; Powlson, D.; Dou, Z. Enhanced-efficiency fertilizers are not a panacea for resolving the nitrogen problem. *Global Change Biology* **2018**, *24* (2), e511−e521.
(29) Modolo, L. V.; da-Silva, C. J.; Brandão, D. S.; Chaves, I. S. A minireview on what we have learned about urease inhibitors of agricultural interest since mid-2000s. *J. Adv. Res.* **2018**, *13*, 29−37.
(30) Cantarella, H.; Otto, R.; Soares, J. R.; Silva, A. G. d. B. Agronomic efficiency of NBPT as a urease inhibitor: A review. *J. Adv. Res.* **2018**, *13*, 19−27.
(31) Mazzei, L.; Cianci, M.; Contaldo, U.; Musiani, F.; Ciurli, S. Urease inhibition in the presence of N-(n-butyl) thiophosphoric triamide, a suicide substrate: structure and kinetics. *Biochemistry* **2017**, *56* (40), 5391−5404.
(32) Mazzei, L.; Cianci, M.; Contaldo, U.; Ciurli, S. Insights into Urease Inhibition by N-(n-Butyl) Phosphoric Triamide through an Integrated Structural and Kinetic Approach. *J. Agric. Food Chem.* **2019**, *67* (8), 2127−2138.
(33) Bremner, J. M. Recent research on problems in the use of urea as a nitrogen fertilizer. *Fert. Res.* **1995**, *42*, 321−329.
(34) Zanin, L.; Tomasi, N.; Zamboni, A.; Varanini, Z.; Pinton, R. The urease inhibitor NBPT negatively affects DUR3-mediated uptake and assimilation of urea in maize roots. *Front. Plant Sci.* **2015**, *6* (116), 1007−1018.
(35) Zanin, L.; Venuti, S.; Tomasi, N.; Zamboni, A.; De Brito Francisco, R. M.; Varanini, Z.; Pinton, R. Short-term treatment with the urease inhibitor N-(n-butyl) thiophosphoric triamide (NBPT) alters urea assimilation and modulates transcriptional profiles of genes involved in primary and secondary metabolism in maize seedlings. *Front. Plant Sci.* **2016**, *7* (62), 845−861.
(36) Wang, Y.; Jin, X.; He, L.; Zhang, W. Inhibitory effect of thiourea on biological nitrification process and its eliminating method. *Water Sci. Technol.* **2017**, *75* (12), 2900−2907.
(37) Zacherl, B.; Amberger, A. Effect of the nitrification inhibitors Dicyandiamide, nitrapyrin and thiourea onNitrosomonas europaea. *Fert. Res.* **1990**, *22* (1), 37−44.
(38) Purakayastha, T. J.; Katyal, J. C. Evaluation of compacted urea fertilizers prepared with acid and non-acid producing chemical additives in three soils varying in pH and cation exchange capacity; I. NH3 volatilization. *Nutr. Cycling Agroecosyst.* **1998**, *51* (2), 107−115.
(39) Purakayastha, T. J.; Katyal, J. C. Evaluation of compacted urea fertilizers prepared with acid and non-acid producing chemical additives in three soils varying in pH and cation exchange capacity; II. Yield and N use efficiency by rice. *Nutr. Cycling Agroecosyst.* **1998**, *51* (2), 117−121.
(40) Bremner, J. M.; Douglas, L. A. Decomposition of Urea Phosphate in Soils1. *Soil Sci, Soc, Am, J.* **1971**, *35* (4), 575−578.
(41) Moawad, H.; Enany, M. H.; El-Din, S. M. S. B.; Mahmoud, S. A. Z.; Gamal, R. F. Transformations and effects of urea derivatives in soil. *Z. Pflanzenernaehr. Bodenkd.* **1984**, *147* (6), 785−792.
(42) Fenn, L. B.; Hossner, L. R. Ammonia Volatilization from Ammonium or Ammonium-Forming Nitrogen Fertilizers. In *Advances*

DOI: 10.1021/acssuschemeng.9b02607
ACS Sustainable Chem. Eng. 2019, 7, 13369−13378

in Soil Science; Stewart, B. A., Ed.; Springer: New York, NY, 1985; pp 123−169.
(43) Fenn, L. B.; Richards, J. Ammonia loss from surface applied urea-acid products. *Fert. Res.* **1986**, *9* (3), 265−275.
(44) Von Rheinbaben, W. Effect of magnesium sulphate addition to urea on nitrogen loss due to ammonia volatilization. *Fert. Res.* **1987**, *11* (2), 149−159.
(45) Honer, K.; Kalfaoglu, E.; Pico, C.; McCann, J.; Baltrusaitis, J. Mechanosynthesis of Magnesium and Calcium Salt−Urea Ionic Cocrystal Fertilizer Materials for Improved Nitrogen Management. *ACS Sustainable Chem. Eng.* **2017**, *5* (10), 8546−8550.
(46) Honer, K.; Pico, C.; Baltrusaitis, J. Reactive Mechanosynthesis of Urea Ionic Cocrystal Fertilizer Materials from Abundant Low Solubility Magnesium- and Calcium-Containing Minerals. *ACS Sustainable Chem. Eng.* **2018**, *6* (4), 4680−4687.
(47) Sharma, L.; Kiani, D.; Honer, K.; Baltrusaitis, J. Mechanochemical Synthesis of Ca- and Mg-Double Salt Crystalline Materials Using Insoluble Alkaline Earth Metal Bearing Minerals. *ACS Sustainable Chem. Eng.* **2019**, *7* (7), 6802−6812.
(48) Casali, L.; Mazzei, L.; Shemchuk, O.; Sharma, L.; Honer, K.; Grepioni, F.; Ciurli, S.; Braga, D.; Baltrusaitis, J. Novel Dual-Action Plant Fertilizer and Urease Inhibitor: Urea·Catechol Cocrystal. Characterization and Environmental Reactivity. *ACS Sustainable Chem. Eng.* **2019**, *7* (2), 2852−2859.
(49) Casali, L.; Mazzei, L.; Shemchuk, O.; Honer, K.; Grepioni, F.; Ciurli, S.; Braga, D.; Baltrusaitis, J. Smart urea ionic co-crystals with enhanced urease inhibition activity for improved nitrogen cycle management. *Chem. Commun. (Cambridge, U. K.)* **2018**, *54* (55), 7637−7640.
(50) Sheldrick, G. M. Crystal structure refinement with SHELXL. *Acta Crystallogr., Sect. C: Struct. Chem.* **2015**, *71*, 3−8.
(51) Dolomanov, O. V.; Bourhis, L. J.; Gildea, R. J.; Howard, J. A. K.; Puschmann, H. OLEX2: a complete structure solution, refinement and analysis program. *J. Appl. Crystallogr.* **2009**, *42* (2), 339−341.
(52) Macrae, C. F.; Edgington, P. R.; McCabe, P.; Pidcock, E.; Shields, G. P.; Taylor, R.; Towler, M.; van de Streek, J. Mercury: visualization and analysis of crystal structures. *J. Appl. Crystallogr.* **2006**, *39* (3), 453−457.
(53) Griess, P. Bemerkungen zu der Abhandlung der HH. Weselsky und Benedikt, ‚Ueber einige Azoverbindungen. *Ber. Dtsch. Chem. Ges.* **1879**, *12* (1), 426−428.
(54) Gornall, A. G.; Bardawill, C. J.; David, M. M. Determination of serum proteins by means of the biuret reaction. *J. Biol. Chem.* **1949**, *177* (2), 751−766.
(55) Blakeley, R. L.; Webb, E. C.; Zerner, B. Jack bean urease (EC 3.5.1.5). A new purification and reliable rate assay. *Biochemistry* **1969**, *8* (5), 1984−1990.
(56) Hyman, M. R.; Kim, C. Y.; Arp, D. J. Inhibition of ammonia monooxygenase in Nitrosomonas europaea by carbon disulfide. *J. Bacteriol.* **1990**, *172* (9), 4775−4782.
(57) Hyman, M. R.; Wood, P. M. Methane oxidation by *Nitrosomonas europaea*. *Biochem. J.* **1983**, *212* (1), 31−37.

DOI: 10.1021/acssuschemeng.9b02607
ACS Sustainable Chem. Eng. 2019, 7, 13369−13378